Virus Genes (2010) 40:119–129
DOI 10.1007/s11262-009-0415-5

Transgenic expression of *tomato bushy stunt virus* silencing suppressor P19 via the pOp/LhG4 transactivation system induces viral-like symptoms in tomato

Ran Stav · Anat Hendelman · Kobi Buxdorf · Tzahi Arazi

Received: 15 September 2009 / Accepted: 12 October 2009 / Published online: 27 October 2009

Abstract During natural infection, the *Tomato bushy stunt virus* (TBSV) silencing suppressor protein P19 is expressed at high levels, which are required for optimum viral pathogenicity and silencing suppression. To date, expression of P19 in transgenic host plants has failed to achieve comparable expression levels and thus has provided only limited information on its *in planta* effects. To obtain high P19 expression and study its effects on host plant development in the absence of virus infection, we generated HA-tagged P19 (P19HA)-transgenic tomato reporter plants using the pOp/LhG4 transactivation system, which separates transformation from transgene expression. Upon reporter plant activation with a strong constitutive promoter, the transactivated F1 plants expressed high levels of a functional P19HA protein and displayed multiple abnormal phenotypes, some of which were highly reminiscent of the symptoms described previously for TBSV-infected tomato. Moreover, phenotype severity correlated with P19HA expression level, amount of bound miRNA/miRNA* duplexes, and accumulation of miRNA target transcripts. Together our results demonstrate that the tomato miRNA pathway is markedly compromised by P19, in particular when this protein is relatively abundant, as occurs during natural infection. We suggest that such interference with endogenous silencing may be responsible for at least some of the symptoms characteristic of TBSV-infected tomato.

Electronic supplementary material The online version of this article (doi:10.1007/s11262-009-0415-5) contains supplementary material, which is available to authorized users.

R. Stav · A. Hendelman · K. Buxdorf · T. Arazi (✉)
Institute of Plant Sciences, Agricultural Research Organization, The Volcani Center, P.O. Box 6, 50250 Bet Dagan, Israel
e-mail: tarazi@agri.gov.il

Keywords RNAi suppressor · *Tomato bushy stunt virus* (TBSV) · P19 · miRNA · Tomato · Development

Introduction

Post-transcriptional gene silencing (PTGS) is a conserved biological response to double-stranded (ds) RNAs that regulate through different, but overlapping pathways, endogenous gene expression as well as defense against viruses [1]. PTGS is mediated by small interfering RNAs (siRNAs) and structurally related micro-RNAs (miRNAs), which guide the sequence-specific degradation of complementary RNAs [1]. To ensure successful systemic invasion of a host plant, a common strategy of plant viruses against PTGS is the production of suppressor proteins (VSRs) that interfere with one or more steps of the anti-viral PTGS pathway [2]. When such a step is shared by the miRNA-mediated PTGS pathway, silencing-suppression activity might also inhibit miRNA functions and deregulate the expression of miRNA target genes [3, 4]. As numerous miRNA target genes are transcription factors that function in plant growth and development [5], miRNA suppression is likely to lead to developmental defects in infected plants [2], some of which may resemble symptoms of virus-infected plants [6]. Accordingly, many VSRs were originally identified as symptom determinants that often contributed significantly to the onset of viral disease symptoms [2, 7]. For example, in the case of the potyviral silencing suppressor P1/HC-Pro [8–10], studies have demonstrated that developmental aberrations (i.e., symptoms) of *Potyvirus*-infected plants are associated at least in part with P1/HC-Pro suppressor activity, which perturbs the miRNA silencing pathway [4, 6, 11] and alters the expression of miRNA-regulated genes [4, 6].

Tombusviruses encode a conserved ~19 kDa VSR, termed P19 ([12–14], and reviewed by Scholthof [15]). Like other VSRs, P19 was previously identified as a pathogenicity factor required for the systemic spread of *Tomato bushy stunt virus* (TBSV) in certain hosts [9, 16, 17] and as a symptom determinant [18], but only when produced at its normal high levels [19, 20]. Functional [21, 22] and structural [23, 24] studies established that P19 is a high-affinity short (19–21 nt) dsRNA-binding protein and that dimers of P19 bind siRNA duplexes in a 1:1 stoichiometric ratio. This binding prohibits bound duplexes from unwinding and programming the RNA-induced silencing complex (RISC) [25]. As a consequence, RISC-mediated degradation of cognate viral RNAs [21] is repressed. Moreover, it was shown that transgenic expression of wild-type TBSV P19 [26] and Hemagglutinin (HA)-tagged P19 (P19HA) [4, 27] in *Arabidopsis thaliana* induces the accumulation of several miRNA target transcripts, resulting in vegetative and reproductive developmental phenotypes. In addition, immunoprecipitation analysis showed that P19HA binds to miRNA/miRNA* duplexes [4, 27]. Thus, the potential of P19 to perturb the miRNA pathway and as a result disrupt plant development was established, but only in *A. thaliana*, a non-TBSV host. In contrast, similar efforts to characterize the effects of transgenic P19 in *Nicotiana benthamiana*, an experimental host, resulted in only minor phenotypes, most likely due to P19's low expression levels [22, 28] which failed to mimic the high levels of this protein upon infection with the corresponding virus.

In this study, we describe an original transgenic TBSV P19 expression system, based on the pOp/LhG4 transactivation system [29]. This system enabled strong expression of this VSR in tomato, a natural host for TBSV. We characterized the phenotypes induced by P19 expression and suggest a possible link between P19 suppression activity, developmental aberrations, and TBSV disease symptoms in tomato.

Materials and methods

Plasmid construction

To obtain a P19HA reporter construct, the coding region of TBSV P19 was PCR-amplified with the primers P19-*Xho*I-F (5′-CCGCTCGAGATGGAACGAGCTATACAAGGAAAC-3′) containing a *Xho*I site (underlined) at its 5′-end, and P19-*Bam*HI-HA-R (5′-CGGGATCC*TCA***GGCATAGTCAGGAACATCGTATGGGTA**CTCGCTTTCTTTTTCGAAGGTCTC-3′) containing a *Bam*HI site (underlined), a stop codon (italicized) and 27 bp encoding YPYDVPDYA HA-tag (bold). After sequence verification, the amplified fragment was cloned into the *Xho*I/*Bam*HI sites of the pOp-TATA-BJ36 shuttle vector between an *Op* array [30] and *Agrobacteriumtumefaciens* octopine synthase terminator (OCS) to generate pOp-P19HA. The *Not*I fragment of the pOp-P19HA vector was then mobilized into the binary vector pART27 [31] to generate pART27-pOp:P19HA.

Agroinfiltration of *N. benthamiana* leaves

Appropriate binary plasmids were first electroporated into *A. tumefaciens* (strain GV 3101), and the resulting bacteria were cultured overnight in Luria–Bertani (LB) medium containing the appropriate antibiotics. Then, bacterial cultures were diluted 1:100 in fresh LB medium containing 10 mM MES pH 5.6 and 20 μM acetosyringone and grown overnight. Cultures were pelleted and resuspended in agroinfiltration buffer (10 mM $MgCl_2$, 10 mM MES pH 5.6, and 150 μM acetosyringone) to a final A_{600} of 1.2. Appropriate bacterial cultures were mixed in a 1:1 (v/v) ratio to a final A_{600} of 0.3 each, and incubated for 3 h at 22°C. Bacterial mixtures were then infiltrated into the young leaves of 3-week-old greenhouse-grown *N. benthamiana* plants. Green fluorescent protein (GFP) fluorescence was photographed in detached leaves with a digital camera using a yellow filter under a long-wave UV lamp (UVP model B100A).

Protein extraction and Western blot analysis

For P19HA expression analysis, total protein samples were prepared from each of three 9-mm diameter infiltrated *N. benthamiana* leaf patches or from 35 mg of tomato leaf ground in 150 μl total protein extraction buffer (67 mM Tris–HCl, 2% w/v SDS). Following grinding, 150 μl of 2× SDS–PAGE loading buffer was added and the mixture was boiled for 10 min and cooled on ice. Cooled homogenate was centrifuged for 10 min at 10000×*g* and the supernatant, containing total leaf proteins, was transferred to a new tube. A 35-μl aliquot of the supernatant was fractionated by SDS–PAGE on a 12.5% polyacrylamide gel. The fractionated proteins were electroblotted onto nitrocellulose membranes and probed with commercial rat anti-HA (1:5,000, Roche) or anti-GFP (1:2,000, Santa-Cruz Biotechnology) monoclonal antibodies.

Plant material and growth conditions

M82 tomato (*Solanumlycopersicum*) plants were grown in 400-ml pots under greenhouse conditions with temperatures ranging between 15 and 22°C in a tuff-peat mix with nutrients. For in vitro culture, seeds were surface-sterilized by treatment with 2% hypochlorite solution for 5 min. After rinsing three times with sterile distilled water, seeds were sown on Murashige and Skoog (MS) culture medium containing 3% (w/v) sucrose and 1% (w/v) phytoagar (Sigma),

pH 5.7. Germination and seedling growth were in a growth chamber with a 16 h light/8 h dark period (photosynthetic photon flux density: 50–70 μmol m^{-2} s^{-1}) at a constant temperature of 22°C. For crosses, closed flowers were emasculated by removal of the petals and stamens and hand-pollinated with the pollen of the 35S:LhG4 driver line. Successful pollination was validated following F1 progeny germination by genomic DNA PCR with the primer pair P19-*Xho*I-F and OCS-R (5′-GAAACCGGCGGTAAGGATCT-3′) to detect the pOp:P19HA transgene and 35S-F (5′-AAACCTCCTCGGATTCCATT-3′) and LhG4-R (5′-CAACACGGTTCGGGATGTAGT-3′) to detect the 35S:LhG4 transgene.

Transformation of tomato plants

The binary vector pART27-pOp:P19HA was transformed into tomato cv. M82 by co-cultivation of cotyledons derived from 14-day-old seedlings with *A. tumefaciens* strain GV 3101, essentially as described by McCormick [32]. Transgenic progeny were selected by germinating sterile seeds on selective medium (1× MS medium, 3% sucrose and 100 mg/l kanamycin), where only transgenic seedlings developed a branched root system. Further validation was performed by genomic DNA PCR with the primer pair P19-*Xho*I-F and OCS-R to detect the pOp:P19HA transgene.

Total RNA extraction and small RNA gel blot analysis

Total RNA was isolated from tomato leaves with TRI reagent (Sigma, MT, USA) according to the manufacturer's protocol. After addition of isopropanol, the RNA extract was incubated overnight at −20°C to enhance the precipitation of low-molecular-weight RNAs. Following an ethanol wash, RNA was resuspended in RNase-free water and kept at −80°C until use. Blot hybridization analysis was performed according to Pall et al. [33]. Radiolabeled probes were made by 5′-end-labeling DNA oligonucleotides complementary to miRNA or miRNA* sequences with [γ-^{32}P]ATP by means of T4 polynucleotide kinase (New England Biolabs, MA, USA). Blots were prehybridized and hybridized with EZ-hybridization solution (Biological Industries, Israel). Hybridization was performed at 40°C overnight. Blots were washed three times at 50°C with washing buffer (2× SSC, 0.1% SDS) and autoradiographed using a phosphoimager (Fujifilm, Japan). Densitometric analysis of hybridization signals was carried out using the Gel Analyzer procedure of the IMAGEJ 1.42q program (http://rsbweb.nih.gov/ij/index.html).

Real-time quantitative RT–PCR analysis

Total RNA samples were treated with RNase-free DNase (Fermentas Life Sciences, Lithuania) to eliminate genomic DNA contamination. The concentration and integrity of the RNA samples were determined by using an ND1000 spectrophotometer (Thermo Scientific, DE, USA) and by gel analysis, respectively. First-strand cDNA was synthesized from 1 μg of total RNA using the Superscript first-strand synthesis system for RT–PCR kit and oligo (dT) primer (Invitrogen, CA, USA) following the manufacture's instructions. An RT-negative control was used to ensure the absence of genomic DNA template in the samples. For real-time quantitative PCR, 4 μl of diluted cDNA was used in a 10-μl PCR containing 200 nM of each primer and 5 μl Platinum SYBR Green qPCR supermix-UDG (Invitrogen, CA, USA). The PCRs were performed in a Rotor-Gene 6000 cycler (Qiagen, MD, USA) with a temperature program starting with 15 min at 95°C, then 40 cycles of 15 s at 96°C, 15 s at 62°C, and 20 s at 72°C. At the end, the melting temperature of the product was determined to verify the specificity of the amplified fragment. PCR products were analyzed using Rotor Gene Series 6000 software version 1.7 (Qiagen, MD, USA). The primers used for real-time quantitative PCR were designed using the Primer3Plus computer program (http://www.bioinformatics.nl/cgi-bin/primer3plus/primer3plus.cgi) as follows: SGN-U326326-F (5′-CCACCATTGACAGATTCATCG-3′) and SGN-U326326-R (5′-GGTGAACGAAGTCGGAAGAG-3′); SGN-U563944-F (5′-CAGGTCCAGCAGTCCTTTCT-3′) and SGN-U563944-R (5′-CGCTGGAAACTTGGTGGTAA-3′); Tip41-F (5′-ATGGAGTTTTTGAGTCTTCTGC-3′) and Tip41-R (5′-GCTGCGTTTCTGGCTTAGG-3′); GAPDH-F (5′-ATGCTCCCATGTTTGTTGTGGGTG-3′) and GAPDH-R (5′-TTAGCCAAAGGTGCAAGGCAGTTC-3′). The relative expression level of *SGN-U563944* mRNA was calculated using the $2^{-\Delta\Delta Ct}$ method normalized to *GAPDH* as a reference gene. The relative expression level of *SGN-U326326* mRNA was calculated using a standard curve method and *TIP41* as a reference gene. Three technical replicates for each biological sample were analyzed.

Affinity purification of P19HA

For affinity purification, 35S≫P19HA-2 leaves (1 g) were ground in liquid nitrogen and thawed in 5 ml lysis buffer (50 mM Tris–HCl, pH 7.4, 100 mM KCl, 2.5 mM $MgCl_2$, 0.1% NP-40, 2× Sigma plant protease inhibitor cocktail). The homogenate was then filtered through four layers of Miracloth (Merck Chemicals Ltd., UK) and centrifuged at 9500×*g* for 15 min at 4°C to pellet cell debris. The supernatant was mixed with 1 ml of pre-equilibrated anti-HA resin (Sigma, Germany), rotated for 1 h at 4°C and loaded onto a column. The flow-through fraction was collected before washing. The column was washed with 10 column volumes of lysis buffer and the last wash fraction was collected for analysis. Bound protein was eluted by

sequential addition of 500 µl of 100 mM glycine–HCl pH 2.5. Each eluted fraction was immediately neutralized with 20 µl of 1.5 M Tris–HCl pH 8.8. RNA was recovered by treatment with proteinase K (0.2 µg/ml; Fermentas Life Sciences, Lithuania) in the presence of 0.5% SDS for 40 min at 37°C, followed by extraction with acidic phenol and phenol:chloroform and ethanol precipitation.

Anthocyanin measurement

The first true leaves from three 24-day-old seedlings were assayed for anthocyanin according to Markham and Ofman [34]. Leaf tissue was harvested, immediately ground in liquid nitrogen, and transferred (100 mg) to Eppendorf tubes, and anthocyanins were extracted in the dark in cold methanol:water:acetic acid (11:5:1, v/v). The extracts were spun at 14000×*g* for 10 min and anthocyanin concentration was determined in the supernatant by measuring A_{530}.

Results

Constitutive expression of HA-tagged TBSV P19 VSR following transactivation in tomato

Strong expression of TBSV P19 protein *in planta* has been reported to be embryonic lethal in *A. thaliana* [27], whereas consistently weak P19 expression has been reported in *Nicotiana* species [28], most likely because of selection against strong P19-expressing transformants. To circumvent potential toxicity problems that may be associated with strong expression of TBSV P19 protein in tomato, we took a new, previously untried approach by utilizing the LhG4/pOp transactivation system [29]. In this system, a reporter line is generated with the transgene of choice under the control of an inactive chimeric promoter (pOp). pOp is activated and drives transgene expression only in the F1 progeny following a cross with a driver line that expresses an artificial pOp activator (LhG4). A P19HA reporter plasmid was constructed by subcloning a PCR-amplified TBSV *P19* with an HA tag at its C terminus behind the pOp array [29] in the binary vector pART27 [31] (Fig. 1a). The functionality of the P19HA reporter plasmid in the presence of the LhG4 activator was tested by performing a GFP-based transient suppression assay [9]. Leaves of *N. benthamiana* were infiltrated with a mixture of *A. tumefaciens* cultures harboring a constitutive GFP-expressing construct (35S:GFP), a GFP hairpin silencing construct (35S:GFP-IR), a pART27-pOp:P19HA reporter construct (pOp:P19HA), and a constitutive pART27-p35S:LhG4-expressing construct (Fig. 1a; 35S:LhG4). As controls for GFP silencing and expression efficiency, the bacteria containing 35S:LhG4 and 35S:GFP-IR plasmids, respectively, were replaced with bacteria harboring an empty pART27 vector. At 3 days post-infiltration, bright green fluorescence was visualized and strong GFP expression was detected in the expression-control sectors (Fig. 1b, 2), and none was detected in the silencing-control sectors (Fig. 1b, 1) indicating strong GFP silencing. Strong fluorescence and GFP protein levels, indicative of a strong silencing-suppression activity, were detected in sectors infiltrated with both pOp:P19HA and 35S:LhG4 (Fig. 1b, 3), demonstrating that transactivation by LhG4 drives the expression of functional P19HA is these sectors. Western blot analysis confirmed that the P19HA protein is expressed in the sectors infiltrated with bacteria harboring 35S:LhG4 (Fig. 1b, 3) and not in the other sectors (Fig. 1b, 1 and 2), indicating that pOp is active only in the presence of the LhG4 activator.

To express P19HA in tomato, the GV 3101 bacteria harboring P19HA reporter plasmids were used to transform M82 cotyledons using a standard procedure [32]. Seven independent regenerated pOp:P19HA tomato T0 reporter lines were grown to set seed. PCR of genomic DNA extracted from kanamycin-resistant T1 seedlings with primers specific for the P19HA transgene confirmed that these lines are indeed transgenic (Fig. 2a). Phenotypic analysis of developing tomato plants suggested that their growth and development is identical to that of the parental M82 tomato and Western analysis confirmed that the P19HA protein is not expressed in these plants (data not shown). To identify strong P19HA-expressing lines, different pOp:P19HA reporter lines were crossed (≫) with a homozygous M82 transgenic tomato driver line (35S:LhG4; kindly provided by Y. Eshed, The Weizmann Institute of Science) expressing the LhG4 behind the CAMV-35S constitutive promoter, and total leaf protein extracts from the 35S≫P19HA F1 plants were then analyzed for the presence of P19HA protein by immunoblot with anti-HA antibody. This analysis detected a band of the expected size for P19HA (20.5 kDa), confirming that LhG4 drives the expression of P19HA in these plants. Results are shown for 35S≫P19HA-2 and 35S≫P19HA-4 plants, representing progeny of strong and weak P19HA reporter lines, respectively. These plants were selected for comparative analysis of the effects of high and low P19HA levels on tomato growth and development (Fig. 2b). No P19HA band was detected in the leaves of the 35S:LhG4 driver line lacking the pOp:P19HA transgene (Fig. 2b, c). PCR analysis of the genomic DNA of 35S≫P19HA-2 and 35S≫P19HA-4 plants further confirmed that P19HA-expressing plants indeed contained both pOp:P19HA reporter and 35S::LhG4 driver transgenes (Fig. 2c).

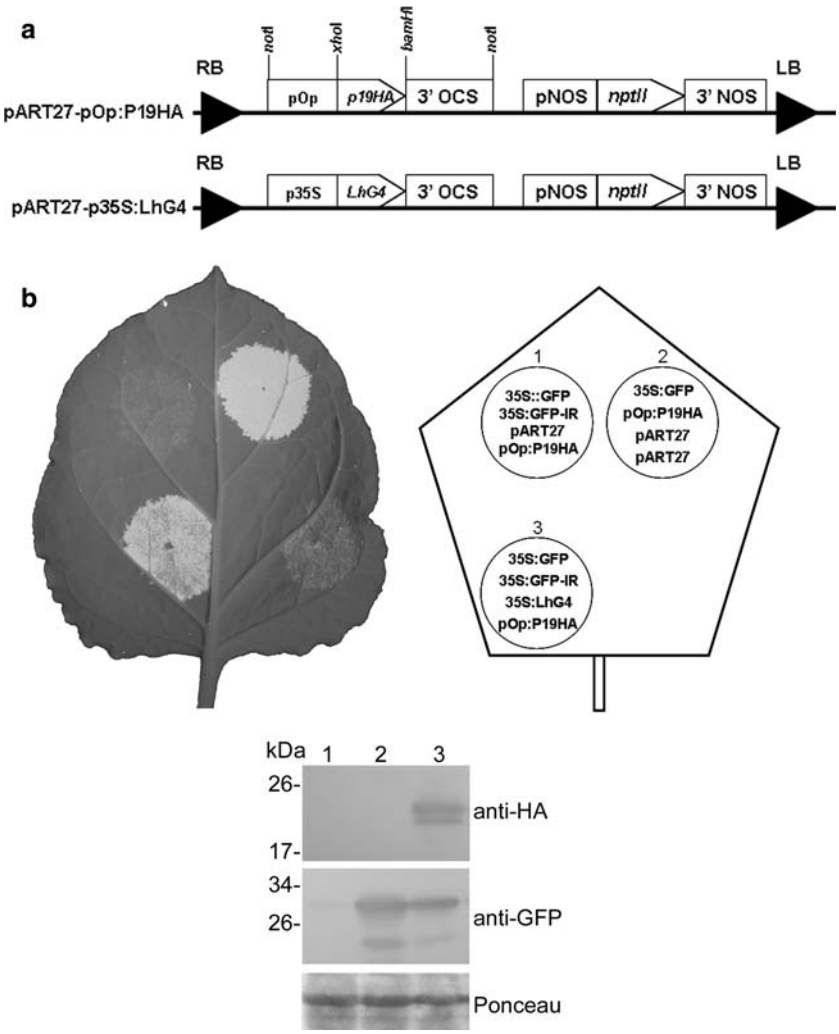

Fig. 1 P19HA suppresses GFP silencing in the presence of LhG4. **a** Schematic representation of the reporter binary plasmid (pART27-pOp:P19HA) used for tomato transformation and in (**b**), and the driver binary plasmid (pART27-p35S:LhG4) [30]. Restriction enzymes used for cloning are indicated. *nptII* a selectable kanamycin-resistance marker, *pOp* eight copies of *lac* operator sequence linked to a minimal *Cauliflower mosaic virus* (CaMV) 35S promoter [29], *p35S* CaMV 35S promoter, *pNOS* nopaline synthase promoter, *3′ NOS* nopaline synthase terminator, *RB* right border, *LB* left border. **b** Suppression of GFP silencing by P19HA upon transient transactivation. *N. benthamiana* leaf sectors were infiltrated with the indicated *A. tumefaciens* mixtures harboring corresponding binary constructs. Photographs were taken under UV light at 3 days post-infiltration, and protein samples were taken at the same time. P19HA and GFP expression levels were detected by Western blotting in equal amounts of total protein extracts (Ponceau), probed with anti-HA or with anti-GFP monoclonal antibodies, respectively. The positions of molecular-mass standards (kDa) are indicated on the left

High levels of P19HA protein perturb the miRNA silencing pathway in tomato

It has been shown that binding of *A. thaliana* miRNA/miRNA* duplexes by P19 stabilizes the normally unstable miRNAs* and increases their cellular steady-state levels [4, 27]. To compare the degree of miRNA* stabilization in strong and weak P19HA-expressing tomato, the levels of previously characterized selected tomato miRNA* [35] were determined in 35S≫P19HA-2 and 35S≫P19HA-4 plants versus control driver plants. RNA gel-blot analysis showed a dramatic increase (up to sixfold) in the levels of SlmiR159*, SlmiR160a*, and SlmiR171a* in the leaves of 35S≫P19HA-2 plants, whereas only SlmiR160a* increased slightly in the leaves of 35S≫P19HA-4 plants which expressed lower P19HA levels (Fig. 3a). Thus, transgenically expressed P19HA probably increased the stability of tomato miRNA/miRNA* duplex via binding and the amount of bound duplexes was directly correlated with the cellular levels of P19HA.

To confirm that P19HA binds directly to tomato miRNAs in vivo, P19HA was affinity-purified from total leaf extracts of 35S≫P19HA-2 plants using a commercial HA-agarose affinity column. The protein content of the eluted fractions was analyzed by immunoblotting, whereas the miRNA content in the E3–E4 fractions was analyzed by

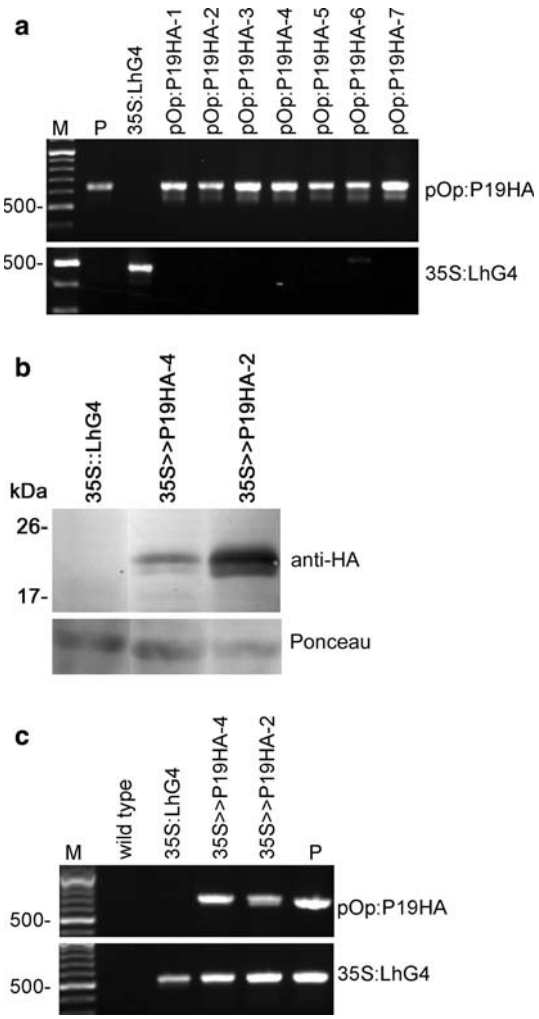

Fig. 2 A cross between pOp:P19HA reporter lines and 35:LhG4 driver plant induces the expression of P19HA protein in the F1 progeny. **a** PCR analysis of tomato pOp:P19HA reporter lines. Genomic DNA was extracted from T1 kanamycin-resistant seedlings (as indicated above) or from the driver line (35S:LhG4) and subjected to PCR with primers specific to pOp:P19HA and 35S:LhG4 transgenes (as indicated). *P* pART27-pOp:P19HA plasmid. **b** Immunoblot analysis of P19HA in leaves of 2-month-old 35S≫P19HA F1 plants (as indicated) or driver (35S:LhG4) tomato plants. Total proteins were extracted from leaves (collected from ten independent plants) and samples (4 μg) were separated by SDS–PAGE (12.5%), blotted, and probed with anti-HA monoclonal antibody. Relative loading of protein in each lane is shown by Ponceau staining. **c** PCR-mediated detection of pOp:P19HA and 35S:LhG4 transgenes in the representative P19HA-expressing F1 plants described in (**b**). Genomic DNA was extracted from 35S≫P19HA F1 plants (as indicated above) or 35:LhG4 driver plant and subjected to PCR with primers specific to pOp:P19HA and 35S:LhG4 transgenes (as indicated). As a negative control, genomic DNA from a wild-type M82 plant was used. *P* plasmids containing either the pOp:P19HA or 35S:LhG4 transgenes

small RNA gel blot analysis alongside total tomato leaf RNA. Analysis of eluted fractions revealed that most of the bound P19HA eluted in the E3 fraction and very little protein eluted in the E4 fraction (Fig. 3b). Northern blot of E3 and E4 fractions detected SlmiR164 in the E3 fraction but not in the E4 fraction (Fig. 3b), suggesting that SlmiR164 co-eluted with the purified P19HA protein, most likely because of direct binding between the two. Unfortunately, we could not test also the binding of SlmiR164* since its sequence is currently unknown.

Binding of miRNA/miRNA* duplex by P19HA is predicted to prevent the bound miRNA from incorporating into RISC and thus to inhibit miRNA-guided cleavage of target transcripts, resulting in an increase in their steady-state cell levels [4, 27]. To validate this prediction in tomato, the steady-state levels of SlmiR164 (*SGN-U326326*) and SlmiR160a (*SGN-U563944*) target transcripts, previously validated by Moxon et al. [35], were quantified from the same leaf RNA sample used for the northern analysis of miRNA*. Real-time quantitative PCR analysis demonstrated a 2.8- to 3.0-fold increase in *SGN-U563944* and *SGN-U326326* transcript levels in 35S≫P19HA-2 compared to 35S:LhG4 driver leaves (Fig. 3c), consistent with the strong increase in miR160a* steady-state levels (Fig. 3a) and the binding of SlmiR164 (Fig. 3b). In contrast, only a weak increase in *SGN-U326326* expression was detected in 35S≫P19HA-4 leaves (Fig. 3c), that expressed low P19HA levels (Fig. 2b). These results indicate that transgenic expression of high P19HA levels causes significant inhibition of SlmiR160a and SlmiR164 activity.

P19HA expression level is correlated with vegetative and reproductive abnormalities

To characterize the effects of differential P19HA levels on tomato development, the phenotypes of 35S≫P19HA-2, 35S≫P19HA-4, and control driver 35S:LhG4 tomato plants were compared from germination till fruit set. Both 35S≫P19HA-2 and 35S≫P19HA-4 seeds germinated normally and seedlings were indistinguishable from controls. Slight growth inhibition was only noticeable at around 17 days post-germination (dpg) in 35S≫P19HA-2 seedlings (Fig. 4). However with time, this growth inhibition was more obvious and accompanied by chlorosis of cotyledons and leaves and accumulation of strong purple color on their abaxial side and around their veins (Fig. 4, 24 dpg). Similar but milder phenotypes were observed at that stage in 35S≫P19HA-4 plants. The purple color observed in the cotyledons and leaves of P19HA-expressing plants suggested the accumulation of anthocyanins. To validate this assumption, the amounts of total anthocyanins were measured in the first true leaves of 35S:LhG4 control, 35S≫P19HA-2 and 35S≫P19HA-4 plants. Increases in anthocyanin content were found in 35S≫P19HA-4 (four-fold) and 35S≫P19HA-2 (5.4-fold) plants compared to control 35S:LhG4 plants (Fig. 4), suggesting that P19HA expression induces anthocyanin accumulation in leaves. At 32 dpg, anthocyanin accumulation, chlorosis, and growth

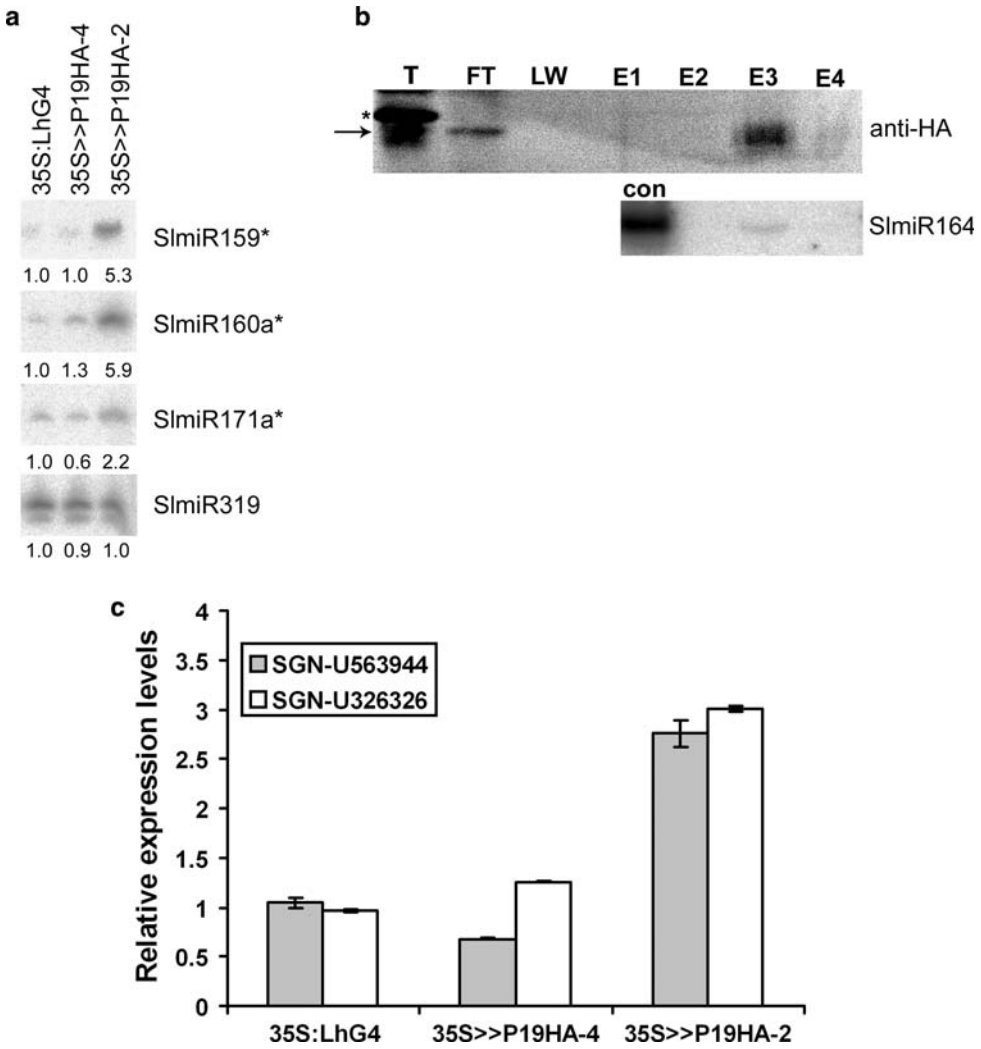

Fig. 3 P19HA binds miRNA/miRNA* duplex and increases the level of their corresponding target mRNAs in 35S≫P19HA-2 tomato leaves. **a** RNA gel blot analysis of indicated SlmiRNAs* and SlmiR319 in leaves of 35S≫P19HA-2, 35S≫P19HA-4 and driver 35S:LhG4 plants. Total RNA was extracted from the same ground leaf mixture used for the immunoblot analysis described at Fig. 2b and identical RNA samples (10 μg) were separated on a denaturing polyacrylamide gel, blotted, and probed with oligonucleotide probes complementary to the indicated SlmiRNAs* or SlmiR319 as a loading control. *Numbers* below each panel refer to accumulation levels relative to the 35S:LhG4 sample (arbitrarily designated as 1.0). **b** Affinity-purified P19HA binds miR164. Total protein extract from 1 g 35S≫P19HA-2 leaves was mixed with an HA-agarose resin (*T*) and loaded on a column. Equal volumes of column effluent fraction (*FT*), final wash fraction (*LW*), and the first to fourth fractions eluted in 100 mM glycine–HCl pH. 2.5 (E1 to E4, respectively) were analyzed for P19HA by immunoblotting with anti-HA antibodies. The positions of P19HA protein and the ~25-kDa light chain of anti-HA monoclonal antibodies are marked by an *arrow* and *asterisk*, respectively. *Bottom panel* RNA was extracted from eluted fractions E3–E4 and subjected to denaturing PAGE, blotted, and probed with an oligonucleotide probe complementary to SlmiR164. Total leaf RNA (12 μg) was used as a SlmiR164 mobility control (con). **c** Quantitative real time RT–PCR analysis of miR160a (*SGN-U563944*) and miR164 (*SGN-U326326*) targets transcripts. The indicated transcripts were quantified in the 35S:LhG4, 35S≫P19HA-4 and 35S≫P19HA-2 total leaf RNA used in (**a**) using primers designed around the corresponding miRNA complementary site and normalized to *GAPDH* or *TIP41* in the sample. mRNA levels relative to 35S:LhG4 are shown. Error bars represent the standard error of three PCR replicates of a single RT reaction

retardation became more severe and were accompanied by crinkling of the strongly anthocyanin-accumulating leaves. In addition, the newly emerging true leaves of 35S≫P19HA-2 seedlings were much smaller and simpler than the control 35S:LhG4 leaves, with rounded instead of serrated margins (Fig. 4). Around 25% of the 35S≫P19HA-2, seedlings did not grow beyond the second true leaf stage, and eventually they shriveled up and died (Fig. 4, arrow). In contrast, all 35S≫P19HA-4 seedlings survived and although their true leaves were simpler, like those of the 35S≫P19HA-2 plants, they exhibited milder growth retardation, leaf chlorosis, and anthocyanin

Fig. 4 Phenotypes of seedlings expressing P19HA. Pictures of 35S≫P19HA-2 and 35S≫P19HA-4 tomato F1 seedlings at different days post-germination (dpg). A representative 35S≫P19HA-2 seedling with a very severe phenotype is marked by an *arrow*. Driver line seedlings (35S:LhG4) at the same developmental stages are shown as a control. Pot size is 7 × 7 cm. The *white box* shows a close up view of primary leaflets. Scale bars: 1 cm. On the right, anthocyanins were extracted from the first true leaf of three independent 24-dpg seedlings and quantified (A_{530}/g FW) by spectrophotometry

accumulation (Fig. 4), suggesting a direct correlation between P19HA expression level and the severity of these phenotypes.

At 3 months post-germination, 35S≫P19HA-2 plants were much smaller and severely stunted compared to the control 35S:LhG4 plants, which had already flowered. Due to the strong stunting, the 35S≫P19HA-2 plants exhibited a bushy architecture (Fig. 5). In addition, their mature fully expanded leaves were smaller and less complex than the control with fewer primary, intercalary, and secondary leaflets (Fig. 5). Moreover, leaflets were downward curled and chlorotic, with a purple tinge around their margins (Fig. 5). The growth of 35S≫P19HA-4 plants was less retarded than that of 35S≫P19HA-2 plants, but they nevertheless developed a bushy phenotype and their leaves were simpler, although less chlorotic or purple (Fig. 5). Both 35S≫P19HA-2 and 35S≫P19HA-4 plants flowered around 1 month later than 35S:LhG4 plants and their flowers had a normal phenotype (data not shown). The flowers of 35S≫P19HA-4 were fertile and ripened into seed-bearing fruits (see Online resource 1 in Supplementary material). However, fruit ripening was observed in only a few cases in 35S≫P19HA-2 plants and developing fruits were smaller than control fruits. When they finally ripened, the fruit had a blotchy color, a relatively well-developed locular tissue and the jelly material contained mostly small seed-like structures that did not germinate (see Online resource 1 in Supplementary material).

Discussion

Transgenic expression of viral silencing-suppressor genes may provide important insights into their effects on plant gene expression and development, especially when expressed in their natural host plants at levels comparable to natural infection. In this study, we characterized the effects of the VSR TBSV P19 on tomato development, in

Fig. 5 Adult phenotype of 35S≫P19HA F1 plants. **a** A comparison of plant architecture of representative 90-day-old tomato driver plant (35S:LhG4) and 35S≫P19HA F1 plants (as indicated), demonstrating stunting and bushiness. The diameter of the pot is 19 cm. **b** Comparative morphology of fully expanded leaf of plants depicted in (**a**) demonstrating reduced leaf complexity and chlorosis; adaxial and abaxial views are shown. Scale bars: 10 cm. *Inset* close-up view of the terminal leaflet's abaxial side. Scale bars: 1 cm

the absence of virus infection, by successfully expressing it at notable levels via the LhG4/pOp transactivation system [29]. The major advantage of this system over standard direct expression systems is that the transgene of choice (here, P19HA) is not expressed in the transgenic reporter plants, thereby avoiding the negative selection which might be exerted against strong transgenic lines. This is especially critical in the case of P19 since lethal symptoms have been observed in *N. benthamiana* plants [18, 36] upon this VSR's high heterologous expression. In addition, previous efforts to transgenically express P19 by direct explant transformation in tissue culture either failed [22], generated only a few T0 transgenic plants that could not be propagated due to sterility [37], or produced plants that expressed very low levels of the P19 protein [22, 28]. The low transgenic P19 expression levels obtained to date are less likely to reflect the degree of endogenous PTGS suppression that a plant experiences during infection since in TBSV-infected cells, the P19 protein is normally expressed at high levels [12, 20], required for its optimum performance and viral pathogenicity [12]. In contrast to previous efforts, the transactivation approach described in this study enabled us to achieve consistently strong P19 expression levels in tomato, thus enabling us to faithfully characterize its effects on tomato from germination till fruit ripening.

When infected with TBSV, tomato plants, which function as natural hosts for this virus, harbor strong symptoms, many of which are manifested as severe developmental aberrations. These include stunting and bushy appearance, a reduction in leaf size and lower leaves that are often curled and chlorotic, with a purple tinge. In addition, fruit yield is greatly reduced and many of them are seedless [38]. We do not know the extent to which the transgenic P19HA expression pattern in 35S≫P19HA plants resembles its expression during tomato TBSV infection; nevertheless, our observations suggest that strong transgenic expression of functional P19HA can mimic key TBSV disease symptoms such as stunting and bushiness, reduction in leaf size, curling, chlorosis, accumulation of anthocyanin around the leaf tip, and fruit sterility (Figs. 4, 5, and Online resource 1 in Supplementary material). Furthermore, around 25% of the strongly expressing 35S≫P19HA-2 seedlings wilted (Fig. 4), which is reminiscent of TBSV infection of young tomato plants that causes wilt due to basal stem necrosis [38]. In addition, phenotype severity was directly correlated with the degree of P19HA expression, in agreement with the fact that TBSV pathogenicity requires high expression levels of P19 in infected cells [20]. Thus, although a direct comparison with TBSV-infected tomato was not done due to restrictions on the use of TBSV in Israel, our results indicate that P19 functions as a TBSV symptom determinant in tomato, when expressed at appropriate levels, in accordance with a similar function in other host plants [15].

P19 blocks viral silencing by directly binding viral siRNAs [21, 22, 39], but can also associate with

structurally similar miRNA duplexes, as demonstrated by immunoprecipitation of P19HA from transgenic *A. thaliana* [4, 27, 40], and by affinity purification in this study (Fig. 3b). In *A. thaliana*, miRNA inactivation due to binding by P19 was correlated with an increase in corresponding mRNA target levels and developmental phenotypes such as stunting, smaller and serrated leaves, flower deformation and reduced fertility [4, 26, 27]. Accordingly, significant inhibition of miRNA activity, as manifested by the elevated levels of miRNA* strands (Fig. 3a) and SlmiR164/160a target transcript accumulation (Fig. 3c), was detected in 35S≫P19HA-2 tomato leaves that displayed severe growth phenotypes (Figs. 4 and 5). In light of the key roles played by miRNAs in plant growth, development and patterning [5], it is likely that such interference with the miRNA pathway will affect certain aspects of 35S≫P19HA-2 development. For example, binding of SlmiR164 by P19HA might reduce leaf complexity as a result of misregulation of miR164-regulated transcription factors and their target genes involved in leaf morphogenesis. Indeed, a reduction in the number of secondary and intercalary leaflets was observed in M82 mutant tomato expressing a miR164-resistant version of *goblet*, a miR164 target that encodes a no apical meristem domain transcription factor, involved in specifying leaflet boundaries in tomato compound leaves [41, 42]. Nevertheless, it was recently demonstrated that TBSVs encoding siRNA-binding mutants of P19 are still able to induce systemic symptoms in *N. benthamiana* and spinach, but not in pepper [36], maybe through interaction with unknown host factors. Thus, we cannot rule out the possibility that at least some of the defects observed in P19HA-expressing tomato plants occur via a similar mechanism.

Like P19, many known VSRs of gene silencing interfere with endogenous silencing pathways [2], and hence might obstruct the generation of strong transgenic lines via explant transformation. Our results suggest that *in planta* expression of a VSR using a transactivation system is a preferred alternative to direct expression, especially if strong expression levels of the VSR are desired. Finally, the pOp:P19HA-2 reporter line described in this study will also be utilized in future research to express P19HA in specific organs and tissues by crossing it with tomato driver lines that express LhG4 through tissue-specific or inducible promoters. Such expression is expected to generate a specific block of endogenous silencing that in turn will enable us to uncover developmental processes and pathways regulated by RNAi in that location.

Acknowledgments We thank the labs of Ori N. and Eshed Y. for their help with the pOp/LhG4 plasmids and for the tomato transformation guidance. We thank Ovadia R. for the anthocyanin measurements. We thank A. Gal-On for critical reading of the manuscript. This is contribution no. 130/2009 series, from the Agricultural Research Organization, the Volcani Center, Israel.

References

1. P. Brodersen, O. Voinnet, Trends Genet. **22**, 268 (2006)
2. O. Voinnet, Nat. Rev. Genet. **6**, 206 (2005)
3. P. Dunoyer, O. Voinnet, Curr. Opin. Plant Biol. **8**, 415 (2005)
4. E.J. Chapman, A.I. Prokhnevsky, K. Gopinath, V.V. Dolja, J.C. Carrington, Genes Dev. **18**, 1186 (2004)
5. D. Garcia, Semin. Cell Dev. Biol. **19**, 586 (2008)
6. K.D. Kasschau, Z. Xie, E. Allen, C. Llave, E.J. Chapman, K.A. Krizan, J.C. Carrington, Dev. Cell **4**, 205 (2003)
7. J.A. Diaz-Pendon, S.W. Ding, Annu. Rev. Phytopathol. **46**, 303 (2008)
8. R. Anandalakshmi, G.J. Pruss, X. Ge, R. Marathe, A.C. Mallory, T.H. Smith, V.B. Vance, Proc. Natl. Acad. Sci. USA **95**, 13079 (1998)
9. G. Brigneti, O. Voinnet, W.X. Li, L.H. Ji, S.W. Ding, D.C. Baulcombe, EMBO J. **17**, 6739 (1998)
10. K.D. Kasschau, J.C. Carrington, Cell **95**, 461 (1998)
11. Y.M. Shiboleth, E. Haronsky, D. Leibman, T. Arazi, M. Wassenegger, S.A. Whitham, V. Gaba, A. Gal-On, J. Virol. **81**, 13135 (2007)
12. W. Qiu, J.W. Park, H.B. Scholthof, Mol. Plant Microbe Interact. **15**, 269 (2002)
13. F. Qu, T.J. Morris, Mol. Plant Microbe Interact. **15**, 193 (2002)
14. O. Voinnet, Y.M. Pinto, D.C. Baulcombe, Proc. Natl. Acad. Sci. USA **96**, 14147 (1999)
15. H.B. Scholthof, Nat. Rev. Genet. **4**, 405 (2006)
16. T. Dalmay, L. Rubino, J. Burgyan, A. Kollar, M. Russo, Virology **194**, 697 (1993)
17. H.B. Scholthof, K.B. Scholthof, M. Kikkert, A.O. Jackson, Virology **213**, 425 (1995)
18. H.B. Scholthof, K.B. Scholthof, A.O. Jackson, Plant Cell **7**, 1157 (1995)
19. K.B. Scholthof, H.B. Scholthof, A.O. Jackson, Virology **211**, 324 (1995)
20. H.B. Scholthof, B. Desvoyes, J. Kuecker, E. Whitehead, Mol. Plant Microbe Interact. **12**, 670 (1999)
21. R. Omarov, K. Sparks, L. Smith, J. Zindovic, H.B. Scholthof, J. Virol. **80**, 3000 (2006)
22. D. Silhavy, A. Molnar, A. Lucioli, G. Szittya, C. Hornyik, M. Tavazza, J. Burgyan, EMBO J. **21**, 3070 (2002)
23. J.M. Vargason, G. Szittya, J. Burgyan, T.M. Hall, Cell **115**, 799 (2003)
24. K. Ye, L. Malinina, D.J. Patel, Nature **426**, 874 (2003)
25. L. Lakatos, T. Csorba, V. Pantaleo, E.J. Chapman, J.C. Carrington, Y.P. Liu, V.V. Dolja, L.F. Calvino, J.J. Lopez-Moya, J. Burgyan, EMBO J. **25**, 2768 (2006)
26. I. Papp, M.F. Mette, W. Aufsatz, L. Daxinger, S.E. Schauer, A. Ray, J. van der Winden, M. Matzke, A.J. Matzke, Plant Physiol. **132**, 1382 (2003)
27. P. Dunoyer, C.H. Lecellier, E.A. Parizotto, C. Himber, O. Voinnet, Plant Cell **16**, 1235 (2004)
28. S.A. Siddiqui, C. Sarmiento, E. Truve, H. Lehto, K. Lehto, Mol. Plant Microbe Interact. **21**, 178 (2008)
29. I. Moore, L. Galweiler, D. Grosskopf, J. Schell, K. Palme, Proc. Natl. Acad. Sci. USA **95**, 376 (1998)
30. J.P. Alvarez, I. Pekker, A. Goldshmidt, E. Blum, Z. Amsellem, Y. Eshed, Plant Cell **18**, 1134 (2006)
31. A.P. Gleave, Plant Mol. Biol. **20**, 1203 (1992)

32. S. McCormick, *Transformation of Tomato with Agrobacterium tumefaciens* (Kluwer Academic Publishers, Dordrecht, The Netherlands, 1991)
33. G.S. Pall, C. Codony-Servat, J. Byrne, L. Ritchie, A. Hamilton, Nucleic Acids Res. **35**, e60 (2007)
34. K.R. Markham, D.J. Ofman, Phytochemistry **34**, 679 (1993)
35. S. Moxon, R. Jing, G. Szittya, F. Schwach, R.L. Rusholme Pilcher, V. Moulton, T. Dalmay, Genome Res. **18**, 1602 (2008)
36. Y.C. Hsieh, R.T. Omarov, H.B. Scholthof, J. Virol. **83**, 2188 (2009)
37. M.L. Alvarez, H.L. Pinyerd, E. Topal, G.A. Cardineau, Plant Mol. Biol. **68**, 61 (2008)
38. D.S. Sutic, R.E. Ford, M.T. Tosic, *Handbook of Plant Virus Diseases* (CRC Press, Boca Raton, 1999)
39. L. Lakatos, G. Szittya, D. Silhavy, J. Burgyan, EMBO J. **23**, 876 (2004)
40. B. Yu, E.J. Chapman, Z. Yang, J.C. Carrington, X. Chen, FEBS Lett. **580**, 3117 (2006)
41. Y. Berger, S. Harpaz-Saad, A. Brand, H. Melnik, N. Sirding, J.P. Alvarez, M. Zinder, A. Samach, Y. Eshed, N. Ori, Development **136**, 823 (2009)
42. T. Blein, A. Pulido, A. Vialette-Guiraud, K. Nikovics, H. Morin, A. Hay, I.E. Johansen, M. Tsiantis, P. Laufs, Science **322**, 1835 (2008)